

**SANDIA REPORT**

SAND2021-15715

Printed December 2021

**Sandia  
National  
Laboratories**

# Discrete Modeling of a Transformer with ALEGRA

Angel E. Rodríguez, John H. Niederhaus, Wesley J. Greenwood, Christopher Clutz Jr.

Prepared by  
Sandia National Laboratories  
Albuquerque, New Mexico  
87185 and Livermore,  
California 94550

Issued by Sandia National Laboratories, operated for the United States Department of Energy by National Technology & Engineering Solutions of Sandia, LLC.

**NOTICE:** This report was prepared as an account of work sponsored by an agency of the United States Government. Neither the United States Government, nor any agency thereof, nor any of their employees, nor any of their contractors, subcontractors, or their employees, make any warranty, express or implied, or assume any legal liability or responsibility for the accuracy, completeness, or usefulness of any information, apparatus, product, or process disclosed, or represent that its use would not infringe privately owned rights. Reference herein to any specific commercial product, process, or service by trade name, trademark, manufacturer, or otherwise, does not necessarily constitute or imply its endorsement, recommendation, or favoring by the United States Government, any agency thereof, or any of their contractors or subcontractors. The views and opinions expressed herein do not necessarily state or reflect those of the United States Government, any agency thereof, or any of their contractors.

Printed in the United States of America. This report has been reproduced directly from the best available copy.

Available to DOE and DOE contractors from  
U.S. Department of Energy  
Office of Scientific and Technical Information  
P.O. Box 62  
Oak Ridge, TN 37831

Telephone: (865) 576-8401  
Facsimile: (865) 576-5728  
E-Mail: [reports@osti.gov](mailto:reports@osti.gov)  
Online ordering: <http://www.osti.gov/scitech>

Available to the public from  
U.S. Department of Commerce  
National Technical Information Service  
5301 Shawnee Rd  
Alexandria, VA 22312

Telephone: (800) 553-6847  
Facsimile: (703) 605-6900  
E-Mail: [orders@ntis.gov](mailto:orders@ntis.gov)  
Online order: <https://classic.ntis.gov/help/order-methods/>



## ABSTRACT

We report progress on a task to model transformers in ALEGRA using the “Transient Magnetics” option. We specifically evaluate limits of the approach resolving individual coil wires.

There are practical limits to the number of turns in a coil that can be numerically modeled, but calculated inductance can be scaled to the correct number of turns in a simple way. Our testing essentially confirmed this “turns scaling” hypothesis.

We developed a conceptual transformer design, representative of practical designs of interest, and that focused our analysis. That design includes three coils wrapped around a rectangular ferromagnetic core. The secondary and tertiary coils have multiple layers. The tertiary has three layers of 13 turns each; the secondary has five layers of 44 turns; the primary has one layer of 20 turns.

We validated the turns scaling of inductance for simple (one-layer) coils in air (no core) by comparison to available independent calculations for simple rectangular coils. These comparisons quantified the errors versus reduced number of turns modeled. For more than 3 turns, the errors are <5%. The magnetic field solver failed to converge (within 5000 iterations) for >10 turns.

Including the core introduced some complications. It was necessary to capture the core surfaces in thin grid sheaths to minimize errors in computed magnetic energy. We do not yet have quantitative benchmarks with which to compare, but calculated results are qualitatively reasonable. They converge on about 380, 320 and 260 times the “air” benchmark values—well within 1 and 5000 (the core relative permeability). The magnetic field solver failed to converge for >7 turns.

Finally, we modeled two coils forming a simple transformer. We demonstrated that ALEGRA can model current induction from a primary to another coil. We simulated both a step-down and a step-up transformer, albeit with crude numbers of turns (4:3 and 3:4, respectively). The simulations match the expected voltage step-down or step-up within 1.6% and 0.32%, respectively. We were able to locate regions of highest electric field ( $\vec{\nabla}\Phi$ ), where arcing is most likely.

## **ACKNOWLEDGEMENTS**

Thanks to Jamie Selander for direction and support. Thanks to Tom Hughes, Chris Siefert, and Allen Robinson for expert assistance with electromagnetics modeling. Thanks to the ParaView and Cubit teams for troubleshooting help. Special thanks to the ALEGRA team for providing the code and troubleshooting help. Finally, a special thank you to Jimmy Carleton for discussions along the way and for reviewing a draft and providing many useful comments and suggestions for improvement.

## CONTENTS

1. Introduction.....	9
2. Test Case: Greenwood Transformer.....	11
3. Validate ALEGRA modeling of a single coil in air.....	13
3.1. Benchmarks .....	13
3.2. ALEGRA Simulations .....	14
3.3. Results.....	15
4. Include the iron core .....	18
4.1. Benchmarks .....	18
4.2. Capture of the core surfaces.....	18
4.3. ALEGRA Results .....	20
5. Two coils — a transformer.....	22
6. Conclusions.....	26
Appendix A. Weaver [11] calculations with wire adjustments .....	29

## LIST OF FIGURES

Figure 1-1 A long solenoid with multiple layers.....	9
Figure 2-1 Greenwood transformer design .....	11
Figure 2-2 Dimensions of windings for Greenwood transformer design.....	11
Figure 2-3 Example simplified Coil and Core.....	11
Figure 2-4 Illustration of "length" for reduced turns .....	12
Figure 3-1 ALEGRA results (symbols) and Weaver calculations for reduced turns (lines).....	15
Figure 3-2 Solutions in Air for 3 turns (upper half) compared to 9 turns (lower half). <b>B</b> magnitude scaled to 20 turns is shown on the $\mathbf{y} = \mathbf{0}$ plane on a log scale.....	17
Figure 4-1 Early solutions with a core for 6 turns (top) compared to 7 turns (bottom). <b>B</b> magnitude scaled to 20 turns is on the $\mathbf{y} = \mathbf{0}$ plane on a linear scale. Equipotential contours are shown on the $\mathbf{y}$ -boundary. The slice through the left-side core shows volume fraction is lower on the outer layers.....	18
Figure 4-2 Elements capturing a body surface emulate Gaussian pillboxes.....	19
Figure 4-3 Improved core gridding. Surfaces are captured in thin layers.....	19
Figure 4-4 Scaled inductance from ALEGRA runs, normalized to benchmark air core values.....	20
Figure 4-5 Growth of grid with cores as number of turns increases .....	20
Figure 4-6 Solutions with improved core gridding for 6 turns (top half) compared to 7 turns (bottom half). <b>B</b> magnitude scaled to 20 turns is on the $\mathbf{y} = \mathbf{0}$ plane on a linear scale. The slice through the left-side core shows the thin layer capturing the core surface.....	21
Figure 5-1 External circuit for two coils .....	22
Figure 5-2 Example primary (red) and two other coils.....	22
Figure 5-3 Voltage and current traces for ALEGRA simulations of 4:3 turns to secondary (blue) and 3:4 turns to tertiary (red).....	23
Figure 5-4 Plots of ALEGRA solutions at second minimum ( $3.5 \mu\text{s}$ ). <b>B</b> magnitude shown on the $\mathbf{y} = \mathbf{0}$ plane. PHI shown on the wires and on a wire-frame outlining one half-core. Left case: 4:3 step-down to same-wound secondary. Right case: 3:4 step-up to counter-wound tertiary.....	24

Figure 5-5 High  $E$  fields near coils for same cases as Figure 5-4.  $E$  magnitude is mapped to greys from transparent white to darkest black. ....24

**LIST OF TABLES**

Table 3-1 Weaver [11] calculations for three rectangular coils .....13  
Table A-2 Weaver [11] calculations with adjusted wires for reduced turns.....29

This page left blank

## ACRONYMS AND DEFINITIONS

Abbreviation	Definition
ALEGRA	Arbitrary Lagrangian-Eulerian General Research Applications
ALE	Arbitrary Lagrangian-Eulerian
MHD	MagnetoHydroDynamics
DC	Direct Current; used as a synonym for “low frequency”



# 1. INTRODUCTION

This document reports progress on a task to study the application of ALEGRA to modeling transformers. ALEGRA is a finite-element Arbitrary Lagrangian-Eulerian (ALE) shock hydrodynamics code with multi-physics options [1]. One of the multi-physics options in ALEGRA is the “Transient Magnetics” option, which assigns electrical conductivity to materials, allows electric current to flow through the domain in accordance with Ohm’s law, and captures electromagnetic induction as well as the transient diffusion of the magnetic field and associated eddy currents. The option includes magnetic and magnetically permeable materials, as well as a fully coupled circuit model. It uses a mimetic spatial discretization scheme with implicit time integration and an iterative Maxwell solver, as described by Bochev et al. (2007) [2].

A transformer transfers electric power from a source through a primary coil to at least one secondary coil and a connected load. The coils are magnetically coupled so an electromotive force is induced in the secondary coil(s), driving current through the load(s). Transient Magnetics can model that induction.

Our purpose is to evaluate how well ALEGRA can model realistic transformers. The goal is a realistic engineering model to quantify such parameters as self-inductance of each coil, mutual inductance and coupling coefficients between coils, and the distribution of magnetic and electric fields, especially maxima of the latter where arcs are likely to begin.

The term “solenoid” usually refers to a long coil, sometimes with more than one winding layer. Most practical solenoids are designed to have a high density of windings, as illustrated in Figure 1-1.

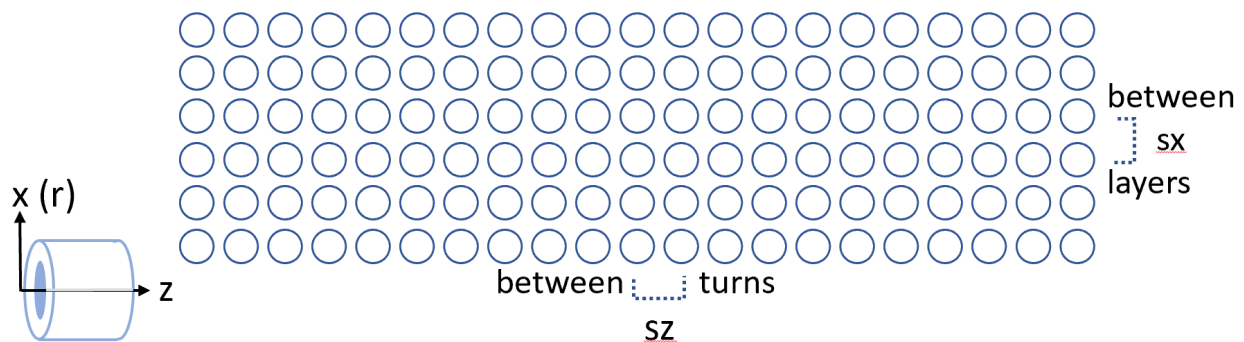


Figure 1-1 A long solenoid with multiple layers

The inductance is an important characteristic of electromagnetic coils. It quantifies the ability of the coil to store energy in the magnetic field, and how it limits the rate of change of current. If an electromotive force  $V$  is suddenly applied across the coil, the current through the coil rises as  $(di/dt) = -V/L$ . Mutual inductance measures the response of one coil to another. Many theoretical predictions for inductance are available in the literature for idealized geometries [3-4]. In this report we study the self-inductance of realistic electromagnetic coils computed by ALEGRA using the Transient Magnetics option, in comparison to independent analytic predictions.

For both mutual and self-inductance, the power-transfer capability depends on the magnitude and spatial arrangement of the magnetic field surrounding the current-carrying circuit elements, and the inductance is directly related to the energy stored in the magnetic field, or the “magnetic energy” (per Equation 3-2, below). This energy is generally insensitive to the details of the current flow in the solenoid itself. The magnetic field is the superposition of contributions from every loop. For many turns, the magnetic energy is dominated by the average current density and cross-sectional area of the solenoids, and the details of individual windings can be ignored. The average current density is given by total current,  $I$ , number of turns,  $N$ , and cross-sectional area of the windings,  $A$ , or in terms of  $s_x$  and  $s_z$ , respectively the layer spacing and winding pitch shown in Figure 1-1, as follows:

$$j_{ave} = \frac{IN}{A} = \frac{I}{s_x s_z} \quad \text{Equation 1-1}$$

Consider greatly increasing the number of turns to a value  $n \gg N$ , while reducing the current in inverse proportion. In the limit as  $n \rightarrow \infty$ , one has a continuous current density model, which is often used as an approximation for a densely wound coil to calculate magnetic energy or inductance either analytically or numerically with good accuracy if the actual number of turns is moderately large.

Rigorously, the contribution of each individual winding to the magnetic field should be computed and superposed with all others to find the total magnetic energy for a given current, and hence the self-inductance. For simple geometries, this “discrete” approach is tractable. For realistic coils with multiple layers and many windings, it is out of reach except for numerical methods. Even with numerical methods, the computational cost of integrating Maxwell’s equations in a medium with a complex arrangement of conductors can be prohibitive [2].

Instead of many turns,  $n \gg N$ , (the correct number), consider approximating the coil with fewer turns,  $n < N$ . The magnetic field for the full winding count can be approximately recovered simply by applying the scaling factor  $N/n$ . This approach maintains a discrete approach with individual windings, but it allows for a computationally tractable problem in ALEGRA. Here we apply this approach for a realistic coil and report its accuracy.

Specifically, we wanted to find out what practical limits there are to modeling discrete coils in ALEGRA, *i.e.* resolving individual wires. Simulations resolving many turns may be impractical. We intend to show that calculated inductance can be scaled from a small number of turns to the correct number within acceptable errors.

We set out to answer these questions:

- 1) How few turns can we get away with and still have reasonable accuracy?
- 2) How many turns can we model without numerical problems or prohibitive computational cost?
- 3) Can ALEGRA demonstrate induction from a resolved primary coil to a secondary?

## 2. TEST CASE: GREENWOOD TRANSFORMER

The geometry of transformer designs can be highly complex [5]. In this study, one of us (Greenwood) developed a transformer geometry that is sufficiently realistic to be representative of engineering design, but hopefully simple enough to supply computational physicists with a reasonable target for analysis. The overall geometry is shown in Figure 2-1. The coils are composed of layers of circular-cross-section copper wires, each forming a rectangular shape with rounded corners wrapped around a central iron core. The design includes a single-layer, 20-turn primary, a 5-layer  $\times$  44 turns secondary, and a 3-layer  $\times$  13 turns tertiary coil. There are 279 windings in total. A polymer encapsulant and insulator layers are part of the design, but they are not analyzed in the models in this work.

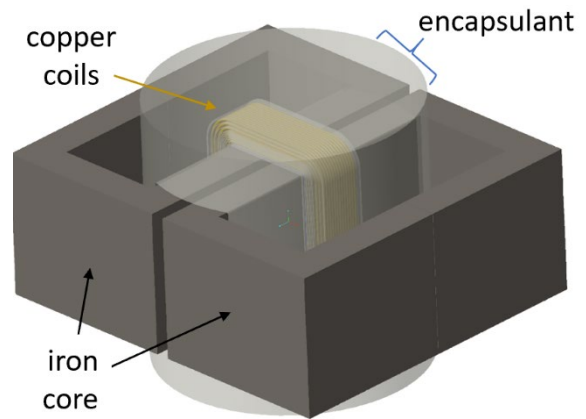


Figure 2-1 Greenwood transformer design

Figure 2-2 shows the key dimensions in mil (0.001 inch) of a cross-section through all the coils.

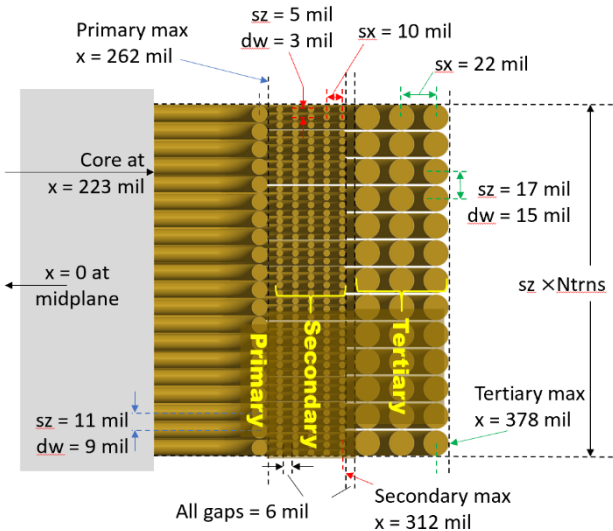


Figure 2-2 Dimensions of windings for Greenwood transformer design

between layers.

Figure 2-3 shows a helical coil and the iron core, as discretized in a hexahedral ALEGRA simulation mesh, depicted by blue gridlines. The mesh is orthogonal and planar, oriented along cardinal cartesian coordinates. That mesh is not conformal to the coil windings, but it is refined where needed to resolve them adequately. Void

We initially ignored the helical nature and tried to link discrete loops in series within ALEGRA, but the large number of circuit model connections required made it impractical. Instead, each coil layer is modeled in a helical arrangement, including the slant angle required to match the pitch between windings. Two of us (Rodriguez and Clutz) converted individual coil layers from the Greenwood geometry into helical coil layers with leads for connectivity. This was done one layer at a time, to avoid the complexities of “cross-over” or “pass-over” connections

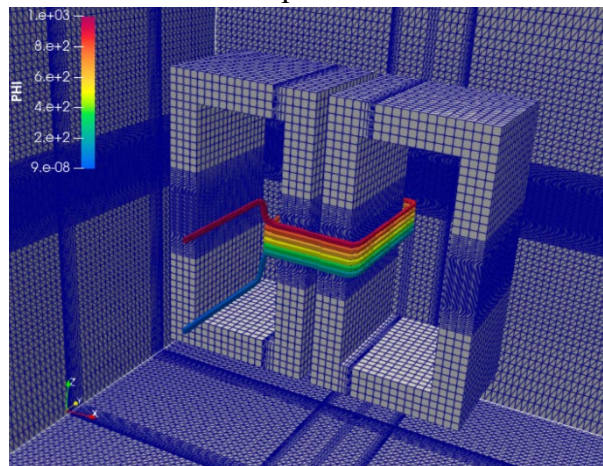
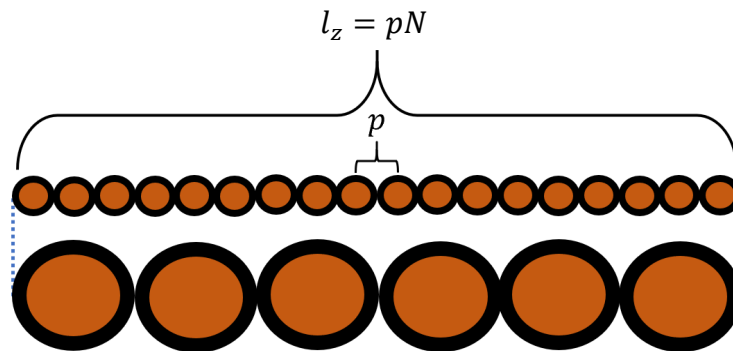


Figure 2-3 Example simplified Coil and Core

regions are not shown. The electric potential (“PHI”) computed by ALEGRA in the final step is shown with colored contours on the coil. The iron core is the two objects resembling cinder blocks. The  $x$  direction is to the right,  $y$  is into the volume, and  $z$  is up. The gap between the blocks is 70 mil (surfaces at  $x = \pm 35$  mil). The  $(x, y, z)$  dimensions of each block are (945, 744, 1752) mil, and the outer thickness of each block is 188 mil on all sides. The coil corner turns are centered on the inner core edges for all coil layers.

The leads go to a domain  $y$  boundary, and the end points are nodes in the external circuit model, which applies a voltage to one node, and the other goes to ground. The grid is refined (denser) in each dimension where necessary to resolve the wires and gaps with at least 4 elements. The boundaries are four cinder block thicknesses away from the blocks or wires. The continuity of PHI confirms that no mixed-material elements produce an extraneous short-circuit in the mesh.

The self-inductance of a coil scales with number of turns as  $N^2$ , as explained in section 3.2. The effects of wire diameter on self-inductance of a coil are less important than coil length. The magnetic induction field,  $\vec{B}$ , around any small wire segment is the same as if the current were on its axis. However, the current through a cross-section of a coil extends to the outside of the first and last wires. For that reason, the coil “length” we kept constant for a reduced number of turns is as illustrated in Figure 2-4. For a given pitch,  $p$  and number of turns,  $N$ , that length is



Equation 2-1

Figure 2-4 Illustration of "length" for reduced turns

### 3. VALIDATE ALEGRA MODELING OF A SINGLE COIL IN AIR

In this section, we report the results of verification runs to compare ALEGRA results to theoretical values for rectangular coils without an iron core. This is often called an air-core coil.

#### 3.1. Benchmarks

Grover (1946) [4] is a comprehensive and widely accepted resource for inductance calculations. Chapter 10 has a formula credited to Y. Niwa [6-7] for rectangular coils, treating each leg as a current sheet. Although the original 1918 and 1924 papers by Niwa are not available, details on the formula and its usage can be found in a more recent study by Rainey *et al.* (2007) [8]. The formula provides the basis of a technique to compute a benchmark value of the self-inductance of any coil layer in the Greenwood transformer geometry, but without an iron core and neglecting the rounded corners of the rectangular coils.

Several online inductance calculators presently exist for rectangular coils using this formula, including at the web addresses listed in references [9-11]. We chose to use the “Rectangular Coil Inductance Calculator” credited to Robert Weaver [11] for generating baseline analytic inductance calculations in this work. This calculator includes the corrections of Rosa [12] for round wires, as well as corrections for skin effect at high frequency. The website provides extensive documentation of the methods used, along with a graphical web interface that performs the calculations for any specific coil geometry. Grover published a thorough critique of these and other methods [13].

The input parameters used in the Weaver calculator for the primary coil and middle layers of the secondary and tertiary coils of the Greenwood geometry are shown along with the output inductance values in Table 3-1. Frequency corrections are small for 500 kHz, as seen in Table 3-1, below the DC values of **L**. The Weaver calculator does not include the effect of current leads or of rounded corner turns. Real leads would be designed to minimize any effect, and the rounded corner turns are assumed to be “tight” enough to have a negligible effect on inductance.

**Table 3-1 Weaver [11] calculations for three rectangular coils**

	<b>Primary (1 layer)</b>	<b>Secondary Layer 3</b>	<b>Tertiary Layer 2</b>		
N	20	44	13		turns
W	0.549	0.615	0.731	in	width
H	0.842	0.908	1.024	in	height
p	0.011	0.005	0.017	in	pitch
p*N	0.22	0.22	0.221	in	length
rw	0.005	0.002	0.008	in	wire radius
dw	0.254	0.1016	0.4064	mm	wire diameter
<b>L</b>	<b>10.8676</b>	<b>60.5819</b>	<b>6.4281</b>	<b>μH</b>	(0 Hz)
	10.8002	60.4314	6.3718	μH	500 kHz

### 3.2. ALEGRA Simulations

ALEGRA simulations were constructed for the Greenwood primary coil and the middle layers of the secondary and tertiary coils. However, the simulations universally failed far short of the full number of turns for each coil, due to non-convergence of the iterative Maxwell solver. This is likely due to the mesh biasing needed to capture the entire magnetized iron core as well as the windings and gaps between them. This biasing produces element aspect ratios and range of element sizes that are known to increase the cost of the Maxwell solve and its likelihood of non-convergence.

However, the inductance is the primary quantity of interest in the simulations, and this allows a pragmatic simplification. The self-inductance  $L$  can be expressed in terms of the coil current,  $I$ , and the volume integral of the magnitude of magnetic field,  $H$ , or induction  $B$ , as follows:

$$L = \frac{1}{I^2} \int \mu H^2 dV = \frac{1}{I^2} \int \frac{B^2}{\mu} dV \quad \text{Equation 3-1}$$

(See equations 2.70-2.73 of Reference [3].) In ALEGRA, the inductance is not computed directly, but rather the total energy stored in the magnetic field, as a discretized volume integral over the entire mesh:

$$E_{mag} = \frac{1}{2} \int \frac{B^2}{\mu} dV \quad \text{Equation 3-2}$$

We confirmed in a few test cases that farther boundaries do not significantly increase the calculated magnetic energy. We obtain the inductance from ALEGRA simulations using the magnetic energy and the tallied current  $I$  as

$$L_{calc} = \frac{2E_{mag}}{I^2} \quad \text{Equation 3-3}$$

The simplification arises because we know that the magnetic induction magnitude  $B$  due to a tightly wound coil is proportional to the number of turns  $N$  (except very near the discrete wires, and those local variations do not significantly affect the total magnetic energy). Therefore, we can say that  $L$  is proportional to  $N^2$ . This means that if we artificially reduce the number of turns in the coil modeled in ALEGRA from  $N$  to  $n$ , as mentioned in Section 1, the inductance of the original coil with the full number of windings can be approximately recovered by

$$L_N = \frac{2E_{mag}}{I^2} \left(\frac{N}{n}\right)^2 = L_{calc} \left(\frac{N}{n}\right)^2 \quad \text{Equation 3-4}$$

If the number of turns modeled is too small, errors (e.g. due to a large pitch angle) may become noticeable.

The ALEGRA simulations are computationally expensive. To keep them to a tractable size for all selected values of  $n$ , while also resolving gaps between windings, it was necessary to adjust the

wire diameter. We adjusted the wire sizes to make the gaps between wires at least equal to the wire diameter. Hence, the modeled wire diameter is at most half the coil pitch, not the actual fraction of pitch, and we ensure that a mesh that resolves the wires also resolves the gaps. By Weaver’s calculator, reducing the wire diameter for the correct number of turns increases the inductance by 0.78%, 0.26% and 1.14% for the modelled primary, secondary and tertiary, respectively. However, we also limited wire radius to 1/3<sup>rd</sup> of the distance from wire center to the core, so that gap would not be smaller than a wire diameter even for few modeled turns. This limitation was most stringent for the primary (closest to the core), but also affected secondary and tertiary for <6 turns. We chose a grid resolution of 4 cells per wire diameter, and relaxed resolution elsewhere.

### 3.3. Results

A set of ALEGRA simulations was conducted for single-layer coils using the Greenwood geometry. Each simulation had one single-layer coil, with no iron core, representing an air background. To test the  $L \propto N^2$  scaling of the self-inductance described above, reduced turns were used, from  $n = 3$  up until simulations aborted. The scaling shown in Equation 3-4 was then used to estimate the inductance of the coil with the full number of turns. The reduced-turns coils were also analyzed using the Weaver calculator [11]. The calculator output for the real coil from Table 3-1 was used as the “Benchmark” value for the data plotted in Figure 3-1. The scaled ALEGRA results are shown in Figure 3-1 as symbols, normalized to the benchmark value. The Weaver calculator output for the reduced coil geometry is also shown with the same normalization, using lines.

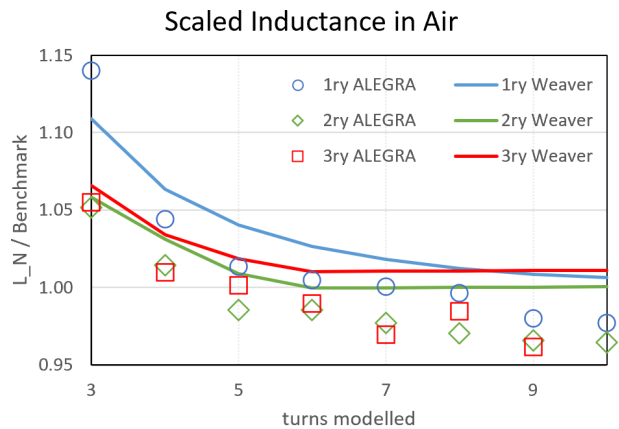


**Figure 3-1 ALEGRA results (symbols) and Weaver calculations for reduced turns (lines).**

The abbreviations 1ry, 2ry and 3ry are used to specify which coil was modeled (by itself). When necessary, we additionally specify which layer, e.g. “2ry/3Lyr”. The Y axis values are normalized to the benchmark values from Table 3-1, so the deviation from 1.00 is a relative error metric (assuming the Weaver benchmarks are accurate). The wire size adjustments for reduced turns is limited so neither the gap between turns nor the gap to the core is smaller than a wire diameter. The expected effect (per Weaver) of those wire size adjustments is shown as the solid lines. The details are in Appendix A. They do not converge to 1 because of the effect of reducing the wire diameter to half the pitch even for the full number of turns—an effect that’s largest for the 13-turn tertiary. The simulation results are comparable, but the ALEGRA results for >7 turns tend toward lower values than Weaver’s. The magnetic field solver fails to converge (within 5000 iterations) for 11 turns (10 for the tertiary).<sup>1</sup> For all successful simulations in Figure 3-1 with more than 3 turns, the scaled inductance computed from ALEGRA results using the reduced-turns approach still match the predictions from Weaver [11] to within less than 5%. This demonstrates the value of the reduced-turns approximation.

<sup>1</sup> This limit may vary for a different gridding.



The Weaver benchmarks may be higher than ALEGRA results because of small differences in the geometries they represent. For example, Weaver does not account for rounded corners on the rectangular windings. If inductance is proportional to the enclosed area, as it is for a simple circular coil, the ALEGRA results should be low in proportion to the reduction in area. Simple geometric calculations for the layers used here indicate that this would produce a deficit of 0.2%, 0.7%, and 1.8% in self-inductance. This might partially, but not completely explain the differences.

The ALEGRA models include simple leads, but Weaver does not. Another possible difference is the magnetic energy “missing” beyond the finite domain of the ALEGRA models. These two differences could not be easily investigated due to the expense of the simulations. Finally, we note that despite the increased thickness of the current path due to the “fat” wires in the ALEGRA models, the current was fully diffused very early in the simulations, so any effect of skin depth is also unlikely to matter very much. Using a sheet current (like Weaver’s first approximation) is a common approximation in analytic solutions, and it is accurate if placed at the true center of the current density.

In any event, errors of 5% and less are reasonable, given the approximations and simplifications. Notice that the trends in Figure 3-1 show convergence to an asymptotic value depends on  $n$ , not on the ratio  $n/N$ . This suggests that a modest number of turns is enough to approximate (after turns scaling) an arbitrarily large correct number,  $N$ , regardless how small the ratio might be.

The calculated inductance and magnetic energy for different numbers of turns depend on the ratio  $B/I$ . The simulations attempt to make the total wire resistance the same for different numbers of turns. However, the simulations do not produce identical currents for different number of turns, because the (unscaled) inductances are different. The currents grow at different rates, but the  $B/I$  ratio approaches an asymptote quickly after initial transients. Therefore, it’s appropriate to compare calculated magnetic induction (“B field” for short) scaled for both turns and current, i.e.:

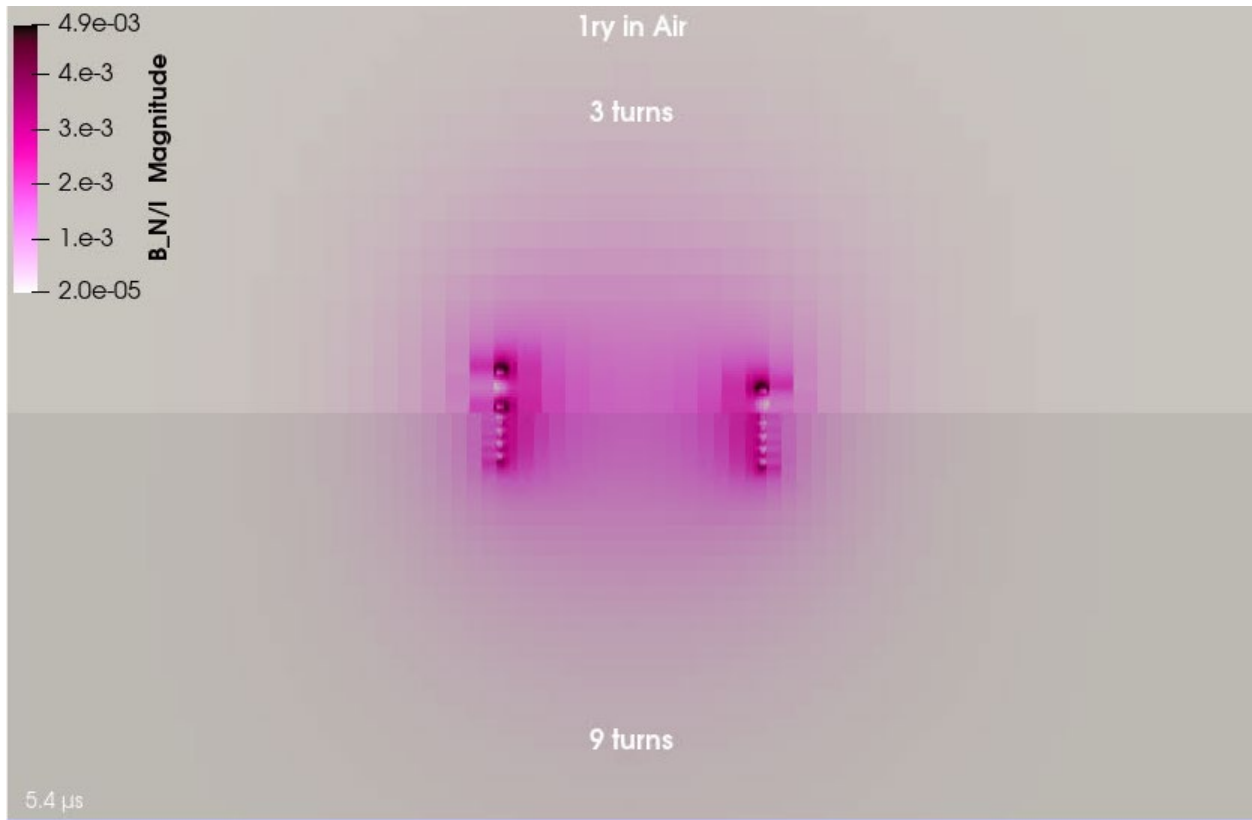
$$\frac{\vec{B}_N}{I} = \frac{\vec{B} N}{I n} \tag{Equation 3-5}$$

Figure 3-2 shows color contours of that scaled field magnitude. The example qualitatively contrasts the primary coil 3-turns solution (+14% error in  $L_N$ ) on the top half with the 9-turns solution (-2% error in  $L_N$ ) on the bottom half. The plot is a slice on the  $y = 0$  plane of symmetry. The differences are obvious near the wires, but decay within a few wire diameters. They only weakly affect the volume integrals that determine scaled inductance or magnetic energy, consistent with the quantitative comparison in Figure 3-1.<sup>2</sup>

---

<sup>2</sup> The 9-turn simulation stopped at 5.4  $\mu$ s, so we made the comparison there.





**Figure 3-2 Solutions in Air for 3 turns (upper half) compared to 9 turns (lower half).  $B$  magnitude scaled to 20 turns is shown on the  $y = 0$  plane on a log scale.**

## 4. INCLUDE THE IRON CORE

The inductance calculation for any coil becomes much more complex with the introduction of a ferromagnetic core. This material acts to concentrate the magnetic flux, making the integral in Equation 3-1 much more difficult to evaluate. No analytic formula or calculator is conceivable for that situation, unless the material fills the entire background. In that case, Equation 3-1 in terms of the magnetic field magnitude  $H = B/\mu$  (which does not change with a change in background  $\mu$ ) shows that the permeability  $\mu$  of the material simply acts as a multiplier on the inductance.

$$L = \frac{1}{I^2} \int \mu H^2 dV \quad \text{Equation 4-1}$$

It was confirmed with ALEGRA in a few test cases that if a coil is embedded in a virtually infinite background with permeability  $\mu > \mu_0$ , the output inductance increases proportionally with  $\mu$ .

The case of a finite ferromagnetic core is more challenging. This is also more realistic, since transformers commonly use high-permeability cores specifically to increase the magnetic flux linkage between coils [5]. For the Greenwood geometry, we chose a relative permeability of  $\mu_{rel} = \mu/\mu_0 = 5000$ , where  $\mu_0$  is the permeability of free space. This value is typical of iron [14]. In practice, transformer cores are built as many thin plates separated by insulation to minimize eddy currents. We mimic this by using an artificially low conductivity of 1 S/m. A typical value for soft iron would be  $10^7$  S/m [15].

### 4.1. Benchmarks

We are unaware of any theoretical solution for a coil with a core like the pair we are modeling. Commercial codes are available that can numerically calculate inductances of arbitrary coil and core geometries. We plan to explore such options in the future. For example, in Reference [16], COMSOL was used to model a transformer and find where high-voltage breakdown might be happening. However, we know the inductance must be bounded by the air-background inductance  $L_{air}$  and the infinite-ferromagnetic-background inductance, which must be  $5000 \times L_{air}$ .

### 4.2. Capture of the core surfaces

Initial simulations of a coil with the core produced anomalies where the scaled inductance did not vary smoothly with the number of turns modeled. Closer inspection showed that the calculated  $B$  field magnitude was

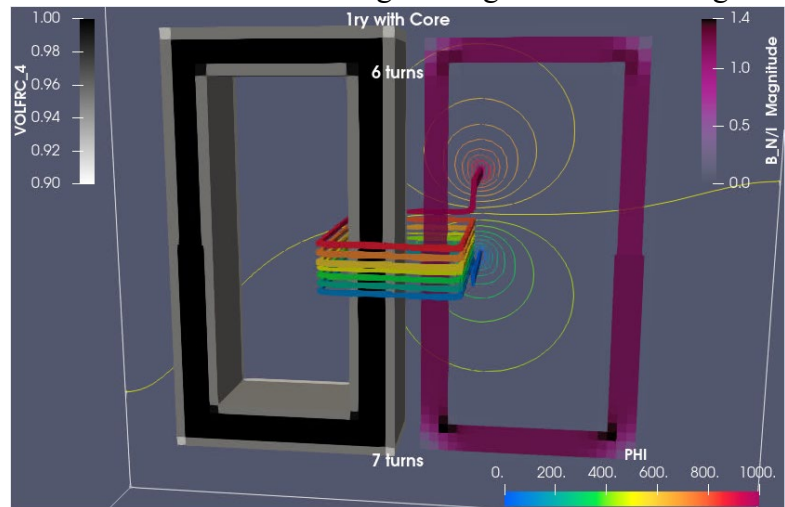


**Figure 4-1 Early solutions with a core for 6 turns (top) compared to 7 turns (bottom).  $B$  magnitude scaled to 20 turns is on the  $y = 0$  plane on a linear scale. Equipotential contours are shown on the  $y$ -boundary. The slice through the left-side core shows volume fraction is lower on the outer layers.**

conspicuously diminished in the sheath of elements at the outer surface of the core, suggesting that the total magnetic energy was being under-estimated. Notice in Figure 4-1 that the width of the magnetized material (magenta on the right) is missing the mixed-material elements (grey on the left), and those widths are noticeably different between 6 and 7 turns. Our meshing scheme indirectly affected the gridding of the core. We limited the largest cell size to  $10 \times$  the smallest size, which is half a wire radius. This changed the core gridding at 7 or more turns, as shown in Figure 4-1. Doubling the nominal core resolution from 4 to 8 per core thickness eliminated the sudden change, but it also produced higher  $L_N$  values (for all  $n$ ), further supporting the hypothesis that magnetic energy was being missed.

This energy loss was due to the known errors in the solution for  $\vec{B}$  that are introduced at material interfaces where there is a discontinuity in  $\mu$ . These errors have been observed in previous work [17], and to avoid them we just need to refine the mesh near the material interface. The meshing scheme was modified accordingly to produce a much finer mesh around the core surface, while still limiting the largest cell size to  $10 \times$  the smallest. This eliminated the anomaly and produced noticeably higher  $L_N$  values for all choices of  $n$ . We believe these are much more realistic results.

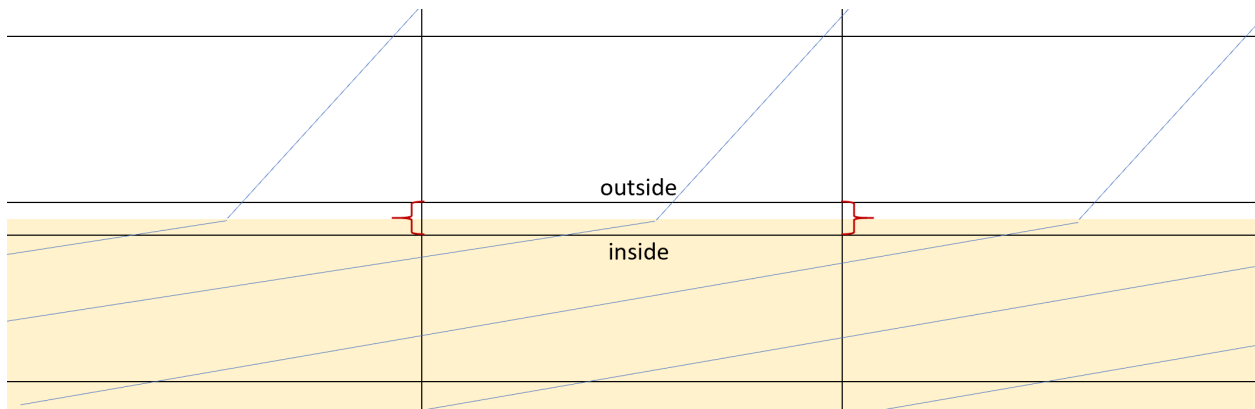


**Figure 4-2 Elements capturing a body surface emulate Gaussian pillboxes.**

Ideally, one would use conformal meshing of the body, and capture the surface discontinuity (in this case, permeability) with Gaussian pillboxes as illustrated in Figure 4-2. Those “pseudo-elements” would have infinitesimal depths, with one face inside the body and the opposite face outside. They could correctly model the field discontinuities, but this would require special handling and algorithm modifications that are not trivial to implement in ALEGRA.

We approximated this approach with thin layers capturing the core surfaces. We made the sizes slightly more than the minimum size that resolves the wires (half a radius), so they would not limit the solver time steps any further. The layers were

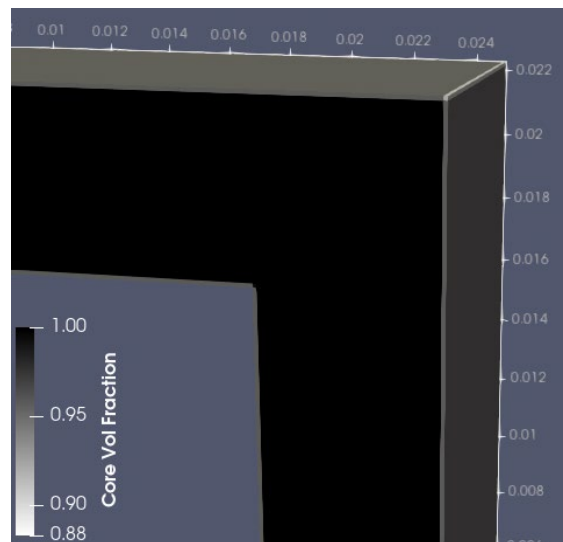


**Figure 4-3 Improved core gridding. Surfaces are captured in thin layers.**

carefully placed to capture mostly core material (>88% volume fractions), as shown in Figure 4-3, above. The plot shows a slice through the middle, to show the pure material (black), in contrast to the thin surface layers (grey).

### 4.3. ALEGRA Results

The ALEGRA results with the core are plotted in Figure 4-4, normalized to the benchmark no-core values. The  $L_N$  values normalized to no-core benchmarks represent the multiplication factor due to the core concentrating the magnetic fields. Those normalized values all fall between the limits of 1 and 5000. The variation with respect to coil number is qualitatively reasonable. The core fills a larger fraction of the volume inside the primary than of any secondary or tertiary layer. The values are reasonably insensitive to reduced number of turns. The primary and secondary 8-turns simulations and the tertiary 7-turns simulations aborted because the magnetic field solver exceeded maximum iterations.

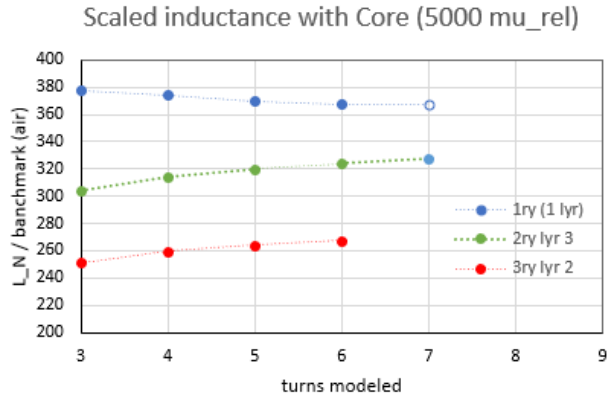


Figure 4-4 Scaled inductance from ALEGRA runs, normalized to benchmark air core values.

The primary 7-turns case initially aborted, but tweaks to the grid made it succeed. The main change was to make the grid largest size  $8 \times$  the smallest, instead of  $10 \times$ , because we suspected the large aspect ratio of outer elements might be causing the magnetic solver aborts. Figure 4-5 shows how the grid grows as we increase number of turns. The empty circles mark the cases with the newer grids. The tiny increase in grid size with the newer grids does not cause noticeable deviations from the trends versus turns.

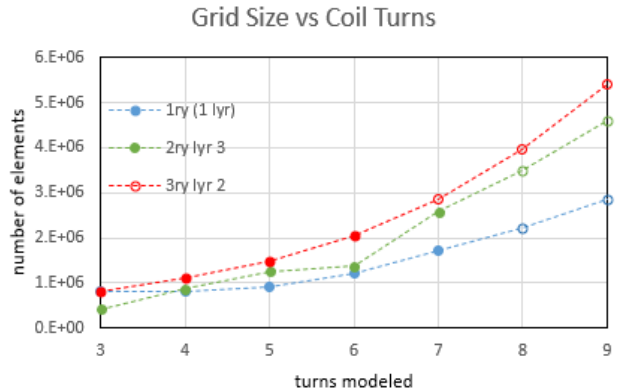
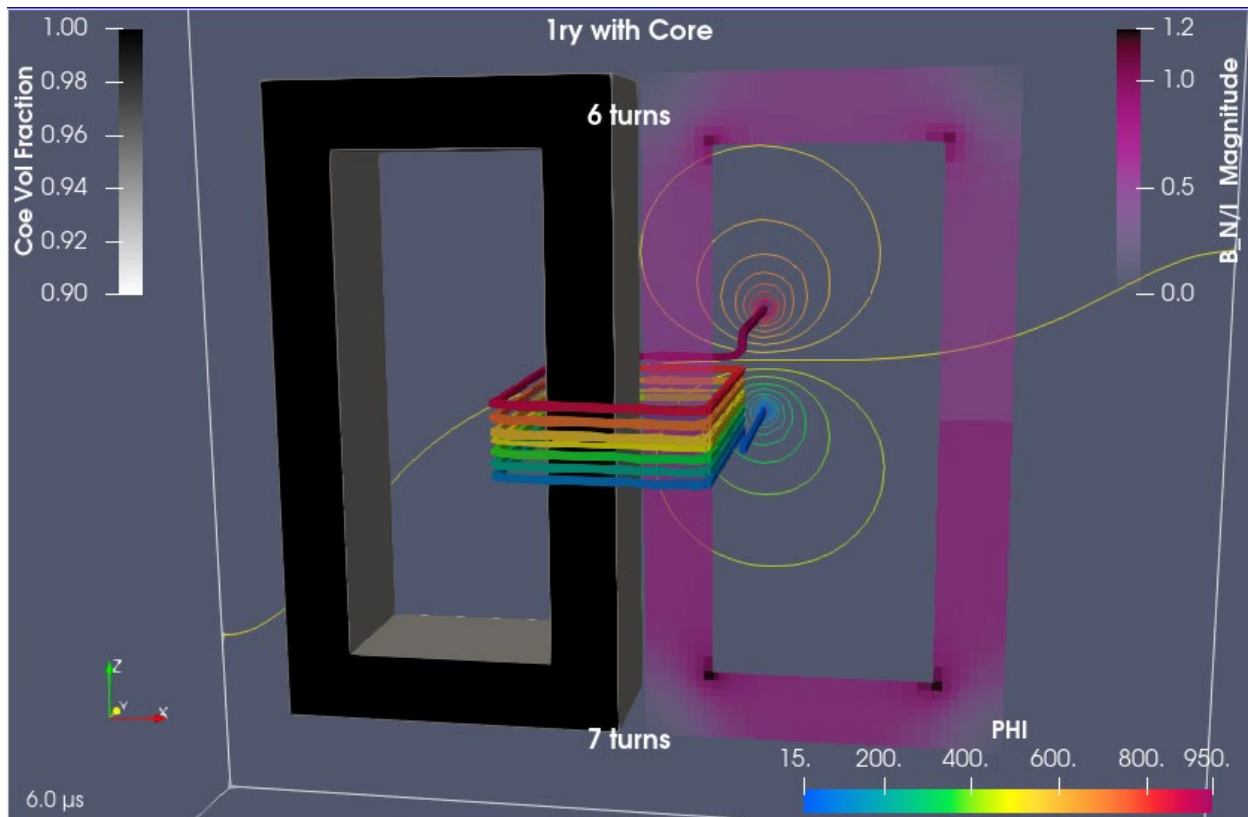


Figure 4-5 Growth of grid with cores as number of turns increases

Figure 4-6 shows calculated  $B$  field magnitudes for the primary with the core, scaled by turns and current ( $B_N/I$ ), comparing 6-turns to 7-turns solutions, just as in Figure 4-1, but after improving the grid. This example compares the primary coil 6-turns solution with the 7-turns solution. With the improved core gridding, the scaled inductances are larger, but 6 vs 7 turn differences in  $B_N/I$  are smaller than in Figure 4-1. With thin grid elements capturing the surface, the mixed-material portions that might be missing magnetic energy become a negligible volume. Also, the improved grid doubled the elements per width, better resolving the  $B$  maxima at the inside corners. The magnetic energy density ( $\propto B^2$ ) is clearly concentrated in the core, so this dominates the inductance. The magnitudes near the wires ( $\sim 0.1$ ) are much less than in the core.



**Figure 4-6 Solutions with improved core gridding for 6 turns (top half) compared to 7 turns (bottom half).  $B$  magnitude scaled to 20 turns is on the  $y = 0$  plane on a linear scale. The slice through the left-side core shows the thin layer capturing the core surface.**

More aggressive limits on largest grid size might succeed in modeling more turns, but at the cost of greatly increasing the number of elements. Even if successful, we suspect we would get diminishing returns.

## 5. TWO COILS — A TRANSFORMER

The third goal is to model a transformer and demonstrate induction in a second coil. The external circuit with two coils is shown in Figure 5-1 for a secondary coil. The  $V_{drv}$  function is a sinusoid of amplitude 1000 V and 2- $\mu$ s period (500 kHz). The current through the resistor from node 22 to 99 is negligible, simulating isolation between the coils. The 1-k $\Omega$  resistor is a dummy load.

We modified the grid to resolve another coil (either secondary or tertiary). Because we have enlarged the wires as part of the reduced-winding scheme, the “fat” wires could overlap for close layers. E.g., the secondary/3Lyr is too close to the primary. To avoid

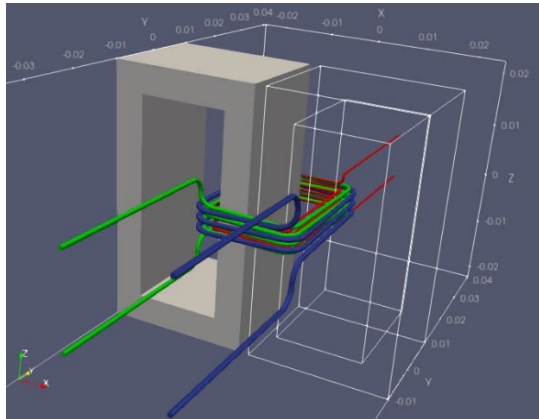


**Figure 5-2 Example primary (red) and two other coils.**

further limits on modeled wire size, we address only the secondary layer 5 (outer-most) and tertiary layer 2 (middle). Three example coils are shown in Figure 5-2, with few turns and fattened wires. As in all one-coil models, one of the leads for each coil is a different material ID, so material masking distinguishes node 11 from node 12, for example. All wires are far enough from each other in all directions. The mesh resolves the quarter-turns enough to avoid any false short circuit through mixed-material elements.

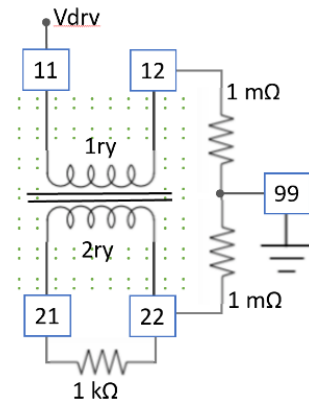


**Figure 5-1 External circuit for two coils**

Secondary and tertiary leads go to the opposite  $y$  boundary as the primary to avoid complications in ALEGRA. If all leads went to the same boundary, either secondary or tertiary coil behaved as if not electrically isolated from the primary. The reasons for this behavior are not understood, since ALEGRA does provide boundary condition options to isolate different leads. The unexpected behavior is avoided here by sending primary leads to a different boundary than the secondary or tertiary leads.

Initially, we naïvely brought the leads of each coil to opposite  $z$  boundaries. This affected the inductance, increasing the errors especially for few turns. The parallel leads better simulate accepted engineering practices, such as using twisted pairs to bring currents to the coils. An alternative would be to omit the leads altogether by using interior surfaces to define the contacts (circuit nodes) and allow current to enter and exit in *ad hoc* fashion at the end points of the coils themselves. ALEGRA allows this, and it may be attempted in future work.

With this setup, we attempt to model (1) a voltage step-down arrangement and (2) a voltage step-up arrangement of coils from the Greenwood geometry. The step-down case uses the reduced Greenwood primary coil with  $n = 4$  and the secondary/5Lyr coil with  $n = 3$ . This 4:3 turns ratio should produce a 25% voltage drop on the secondary coil. The secondary coil is also constructed with opposite polarity to the primary, meaning that the turns are wound in opposite directions— from the top, the primary goes counter-clockwise, but the secondary goes clockwise. Thus, the

voltage output signal on the secondary should be in phase with the primary signal, since the induced current should act to oppose the magnetic flux created by in the primary, by “Lenz’s Law” – see Appendix A in Reference [18].

The step-up case uses the reduced Greenwood primary coil with  $n = 3$  and the tertiary/2Lyr coil with  $n = 4$ . This 3:4 turns ratio should produce a 33% voltage increase on the tertiary coil. The tertiary coil is wound in the same direction as the primary. Thus, its voltage output signal should be 180 degrees out of phase with the primary signal. In both cases, the iron core is included, with the thin grid layers capturing the core surfaces.

The ALEGRA results for these two cases are shown in Figure 5-3. The simulation voltage traces at the top of the figure show that the secondary step-down (blue) and tertiary step-up (red) peaks are close to the expected 750 V and 1333 V, for an input 1000 V signal. The simulation extrema are +768, -752, +691 and -741 V for the step-down case, and -1328, +1330, -1328 and +1330 V for the step-up case. The average unsigned extrema are 738 V for the step-down case, and 1329 V for the step-up case, or 1.6% and 0.32% below the expected 750 and 1333 V, respectively. The secondary signals (blue) are in phase with the input as expected due to the coil polarity, while the tertiary signals (red) are 180 degrees out of phase.

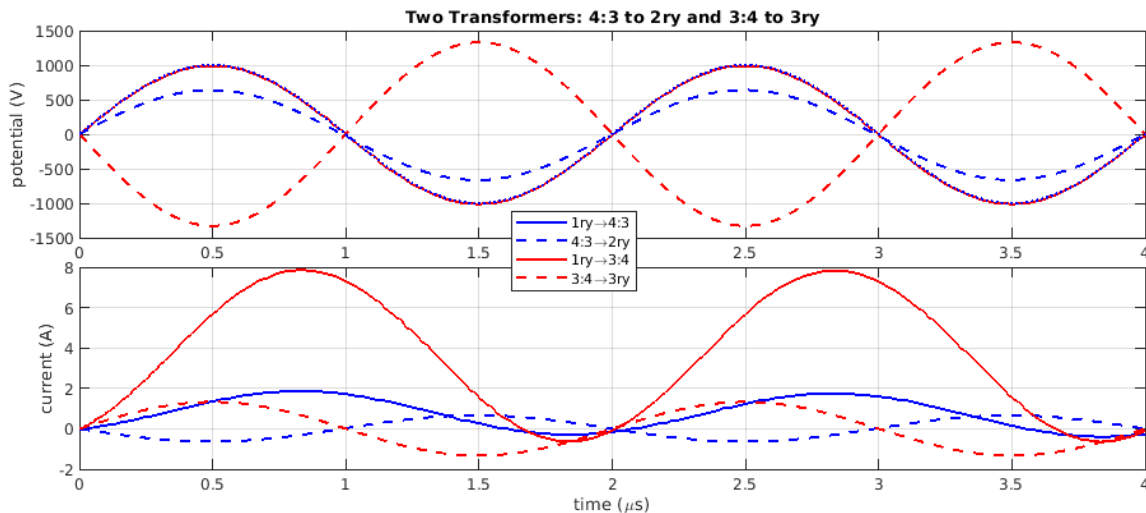


**Figure 5-3 Voltage and current traces for ALEGRA simulations of 4:3 turns to secondary (blue) and 3:4 turns to tertiary (red).**

The corresponding current traces appear on the bottom of Figure 5-3. Inputs to the primary are solid; outputs to the secondary or tertiary are dashed. The input voltages are identical by design, but input currents are different in phase and amplitude because the load impedances are different. The differences in phase and amplitude seen in the current traces is presumably due to these



impedance differences, but that has not been investigated. The asymmetry (DC offset) of the primary current is not understood.

Plots of the calculated fields for the two cases follow in Figure 5-4. The  $B$  fields are clearly concentrated in the cores. A wire frame (feature edges) for one half-core is shown for reference, colored by the electric potential  $\Phi$ , labeled as ‘PHI’. The continuity of PHI colors on the wires confirms that no mixed-material elements provide false short-circuits. Equipotential contours on outer boundaries (not shown) again confirmed that the boundary conditions are reasonable.

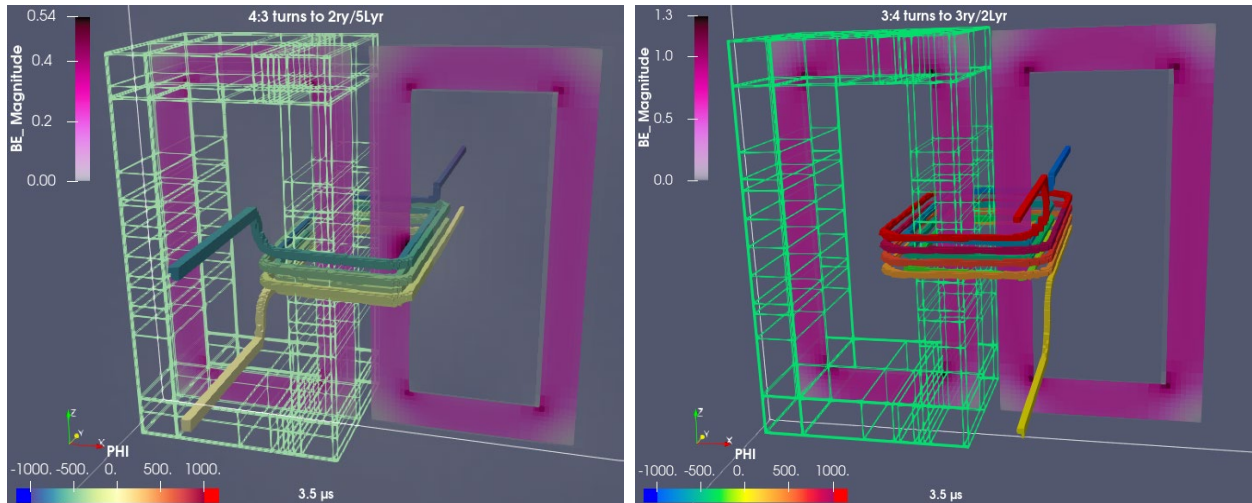


**Figure 5-4 Plots of ALEGRA solutions at second minimum (3.5  $\mu$ s).  $B$  magnitude shown on the  $y = 0$  plane. PHI shown on the wires and on a wire-frame outlining one half-core. Left case: 4:3 step-down to same-wound secondary. Right case: 3:4 step-up to counter-wound tertiary.**

Three-dimensional volume rendering with opacity mapping makes it possible to visualize where the magnitude of the electric field,  $\vec{E} = -\vec{\nabla}\Phi$ , is greatest in the modeled coils for these two cases. The magnitude of  $E$  appears in Figure 5-5 as the smoky haze around the wires. The maximum (blackest) is where arcs are most likely to break down the insulators (not modeled). Since the

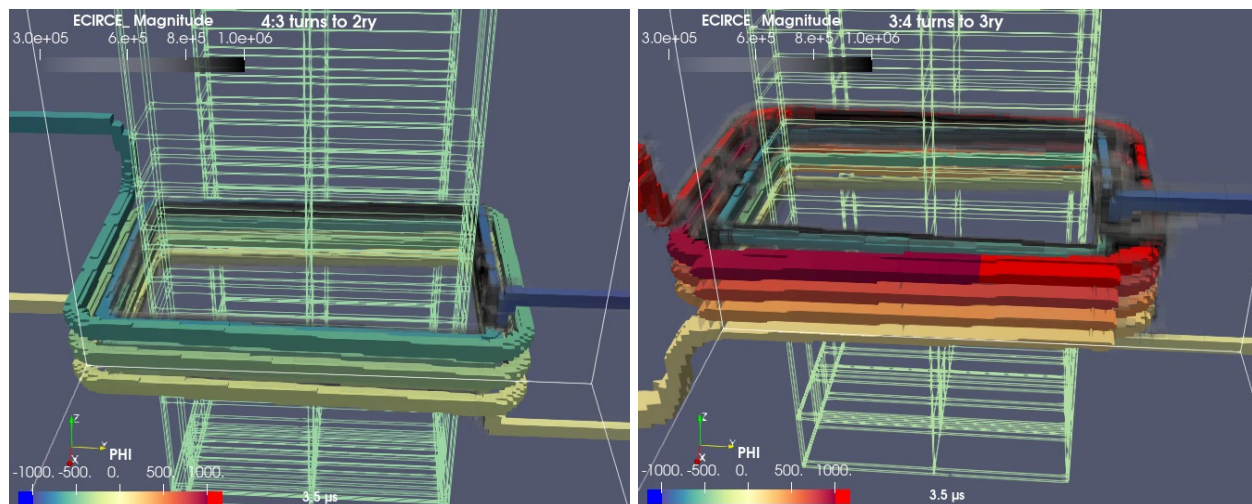


**Figure 5-5 High  $E$  fields near coils for same cases as Figure 5-4.  $E$  magnitude is mapped to greys from transparent white to darkest black.**



secondary is counter-wound to the primary, the potential difference between primary and secondary is minimized. Likely breakdown paths occur between the primary and the core. The core's virtually floating potential tends toward a mean value—the color of the bare wire frame you can see through. In contrast, the potential difference between the primary and tertiary is maximized between the top windings. Hence, likely breakdown paths occur between the primary and tertiary hot ends.

These two examples demonstrate that it is feasible to simulate step-up or step-down transformers in ALEGRA using this approach, albeit with limited numbers of turns.

## 6. CONCLUSIONS

It is possible to resolve coil wires in a numerical simulation, but in practice, there are limits to the number of turns that can be simulated. For the rectangular coil design we studied, ALEGRA was able to simulate single coils in air up to 10 turns. With the core, the limit was 7 turns. With two coils (the primary and one more), the limit may be smaller still.

The simulated inductance can be scaled from few turns to the correct number of turns,  $N$ , because inductance scales as  $N^2$  to good accuracy. In air, the errors for our test case were  $<5\%$  with at least 4 turns, regardless of the total number of turns. When including the core, it was necessary to capture the surfaces in thin layers to minimize errors in computed magnetic energy. Calculated results are qualitatively reasonable, but we do not yet have a quantitative benchmark with which to compare.

We demonstrated that ALEGRA can simulate both a step-down and a step-up transformer, albeit with a small number of turns. Plots of  $E$  field magnitude can be used to locate where electric breakdown is most likely to occur.

## REFERENCES

- [1] A. C. Robinson, T. A. Brunner, S. Carroll, R. Drake, and others, "ALEGRA: An Arbitrary Lagrangian-Eulerian Multimaterial, Multiphysics Code," in: Proceedings of the 46th AIAA Aerospace Sciences Meeting: AIAA-2008-1235, 2008.  
<https://www.doi.org/10.2514/6.2008-1235>
- [2] P. B. Bochev, C. J. Garasi, J. J. Hu, A. C. Robinson, and R. S. Tuminaro, "An improved algebraic multigrid method for solving Maxwell's equations," *SIAM J. Sci. Comput.* **25**(2), pp. 623-642. <https://doi.org/10.1137/S1064827502407706>
- [3] H. Knoepfel, *Pulsed High Magnetic Fields*, North Holland Publishing Co., 1970.
- [4] F. W. Grover, *Inductance Calculations*, D. Van Nostrand Company, 1946. Reprint, Dover, 2009.
- [5] J. W. Coltman, "The Transformer," *IEEE Industry Applications Magazine* **8**(1), January 2002.  
<https://doi.org/10.1109/2943.974352>
- [6] Y. Niwa, (title unknown), Researches of the Electrotechnical Laboratory, Tokyo, No. 73, 1918.
- [7] Y. Niwa, "A study of Coils Wound on Rectangular Frames with Special Reference to the Calculation of the Inductance," Researches of the Electrotechnical Laboratory, Tokyo, No. 141, 1924.
- [8] R. K. Rainey, J. S. DeVries, and B. D. Sykes, *Journal of Magnetic Resonance* **187**(1), 27-27, 2007.  
<https://doi.org/10.1016/j.jmr.2007.03.016>
- [9] "Electrical inductance calculator," <http://www.moshier.net>, accessed October, 2021.
- [10] "Inductance calculation Excel spreadsheet for regular and rectangular solenoidal coils," <http://structbio.biochem.dal.ca/jrainey/downloads.html>, accessed October, 2021.
- [11] "Rectangular Coil Inductance Calculator,"  
<http://electronbunker.ca/eb/InductanceCalcRc.html>, accessed June-October, 2021.
- [12] E. B. Rosa, "Calculation of the Self-Inductance of Single-Layer Coils," *Department of Commerce Bulletin of the Bureau of Standards* **2**(2), pp. 161-187, 1906.  
<https://doi.org/10.6028/bulletin.034>
- [13] F. W. Grover, "A Comparison of the Formulas for the Calculation of Inductance of Coils and Spirals Wound with Wire of Large Cross Section," *Bureau of Standards Journal of Research* **3**(1), pp. 163-190, 1929. <https://doi.org/10.6028/jres.003.016>
- [14] W. F. Brown, "Magnetic Materials," Chapter 8 in the *Handbook of Chemistry and Physics*, Condon and Odishaw, eds., McGraw-Hill, 1958. Referenced from R. Nave, HyperPhysics,  
<http://hyperphysics.phy-astr.gsu.edu>, accessed October, 2021.
- [15] A. M. Helmenstine, "Table of Electrical Resistivity and Conductivity." ThoughtCo.  
<https://www.thoughtco.com/table-of-electrical-resistivity-conductivity-608499>, accessed October, 2021.
- [16] H. Ahn, J. Lee, J. Kim, Y. Oh, S. Jung and S. Hahn, "Finite-Element Analysis of Short-Circuit Electromagnetic Force in Power Transformer," in *IEEE Transactions on Industry Applications*, **47**(3), pp. 1267-1272, 2011. <https://doi.org/10.1109/TIA.2011.2126031>
- [17] M. Grinfeld and J. Niederhaus, "ALEGRA-MHD Simulations for Magnetization of an Ellipsoidal Inclusion," US Army Research Laboratory technical report ARL-TR-8092, 2017.  
<https://apps.dtic.mil/sti/citations/AD1038890>

- [18] T. P. Hughes, “Transient voltage-reversal in transformers with multiple secondary coils”, Sandia National Laboratories technical report SAND2020-7822, July 2020.

## APPENDIX A. WEAVER [11] CALCULATIONS WITH WIRE ADJUSTMENTS

The benchmark inductance values from the Weaver calculator [11] use the actual number of turns and the actual wire diameters, which leave very small gaps between windings. For reduced turns models, the wire diameters,  $dw$ , are modified to make sure neither the gaps between wires nor the gap to the core is smaller. In terms of pitch,  $p$ , and distance from the wire centers to the core surface,  $R_{trn}$ ,

$$dw' = \min(p/2, R_{trn}/3) \quad \text{Equation A-1}$$

Hence, for reduced turns, only pitch and wire diameter are changed among the input values in Table 3-1. Table A-1, below, lists the two adjusted values and the results from the Weaver calculator.

**Table A-2 Weaver [11] calculations with adjusted wires for reduced turns**

turns	dw (mm)			Pitch (in)			L*(N/n)^2 for "fat" wires		
	1ry (1 lyr)	2ry lyr 3	3ry lyr 2	1ry (1 lyr)	2ry lyr 3	3ry lyr 2	1ry (1 lyr)	2ry lyr 3	3ry lyr 2
3	0.287867	0.931333	0.935567	0.073333	0.073333	0.073667	12.05333	64.12462	6.852011
4	0.287867	0.6985	0.701675	0.055	0.055	0.05525	11.5575	62.4602	6.648038
5	0.287867	0.5588	0.56134	0.044	0.044	0.0442	11.304	61.1079	6.548412
6	0.287867	0.465667	0.467783	0.036667	0.036667	0.036833	11.15556	60.55916	6.493825
7	0.287867	0.399143	0.400957	0.031429	0.031429	0.031571	11.06286	60.57309	6.494773
8	0.287867	0.34925	0.350838	0.0275	0.0275	0.027625	11.00188	60.5847	6.495938
9	0.287867	0.310444	0.311856	0.024444	0.024444	0.024556	10.95951	60.5968	6.49732
10	0.2794	0.2794	0.28067	0.022	0.022	0.0221	10.938	60.60842	6.498388
	p/2 (mm)			correct pitch (in)					
	0.254	0.1016	0.4064	<b>0.011</b>	<b>0.005</b>	<b>0.017</b>	<b>10.952</b>	<b>60.7419</b>	<b>6.5014</b>
	<b>0.01397</b>	<b>0.00635</b>	<b>0.02159</b>	20	44	13	<b>10.8676</b>	<b>60.5819</b>	<b>6.4281</b>
	correct dw (mm)			correct N turns					

The last four rows show the calculations for the correct pitch and number of turns for reference. The blue entries are for  $dw = p/2$ ; the bold entries are for the correct wire diameter.

## DISTRIBUTION

### Email—Internal

Name	Org.	Sandia Email Address
Technical Library	01977	<a href="mailto:sanddocs@sandia.gov">sanddocs@sandia.gov</a>

This page left blank

This page left blank





**Sandia  
National  
Laboratories**

Sandia National Laboratories is a multimission laboratory managed and operated by National Technology & Engineering Solutions of Sandia LLC, a wholly owned subsidiary of Honeywell International Inc. for the U.S. Department of Energy's National Nuclear Security Administration under contract DE-NA0003525.